

Spin Density Functional Theory Simulations of Quantum Point Contacts : An Investigation of Spin Filtering Effects

Richard Akis and David Ferry

Department of Electrical Engineering, Arizona State University
Tempe, AZ 85287-5706, USA
richard.akis@asu.edu

ABSTRACT

In this paper, we present simulations of quantum point contacts (QPCs) formed in semiconductor heterostructures over which a metal split-gate has been deposited. Biasing the gates creates a quasi-1D channel (ie. a wire, or a QPC for very short channels) which separates the 2DEG into source and drain regions and through which current can flow. Besides the usual plateaus at integer multiples of $G_0 = (2e^2/h)$, more recent experiments on QPCs however have found additional non-integer plateaus, perhaps the most noteworthy being a $\sim 0.7 G_0$ conductance anomaly. Incorporating spin-density-functional theory (SDFT) into our calculations, we are able to obtain similar anomalies in our simulations. Moreover, we find that these features can be correlated with the formation of a *spin-dependent* energy barrier structure.

Keywords: quantum transport, heterostructures, spin density functional theory, spintronics.

1. INTRODUCTION

Quantum point contacts (QPCs) can be formed in semiconductor heterostructures by depositing metal split-gate. Biasing the gates creates a quasi-1D channel (ie. a wire, or a QPC for very short channels) which separates the 2DEG (two dimensional electron gas) that exists in the heterostructure into source and drain regions and through which current can flow. Measurements have shown that conductance for such structures is quantized with plateaus at integer multiples of $G_0 = (2e^2/h)$ as function of gate voltage[1], a result readily explained by a single electron quantum mechanical theory[2]. More recent experiments however have found additional non-integer plateaus, perhaps the most noteworthy being a $\sim 0.7 G_0$ conductance anomaly that has been observed in QPCs[3] and wires[4]. Theoretically, while there is disagreement about the specifics[5,6], it is generally believed that electron-electron interactions must be included to account for such effects, which can be done by incorporating spin-density-functional theory (SDFT) into the transport calculations.

In this paper, we present our own transport calcula-

tions using SDFT. Besides being able to obtain $\sim 0.7 G_0$ anomalies similar to experiment, we find that these features can be correlated with the formation of *spin-dependent* energy barrier structure which can, in these instances, allow *two modes* of spin-down electrons to be almost fully transmitted through the channel before spin-up electrons start being allowed through. These barriers, which are largely the result of the exchange potential, rise and fall as function of the local density and one can exploit this to tune the spin-filtering effects. For example, varying the density, one can evolve from a $\sim 0.7 G_0$ anomaly to fully formed plateau at $1.0 G_0$, depending on how well the density dependent barrier transmits or blocks the second spin-down mode (spin-up modes are still blocked even in this case). We can also account for additional features such as anomalies at $\sim 0.3 G_0$ and “missing” plateaus at higher conductances, features which have recently been experimentally observed [7].

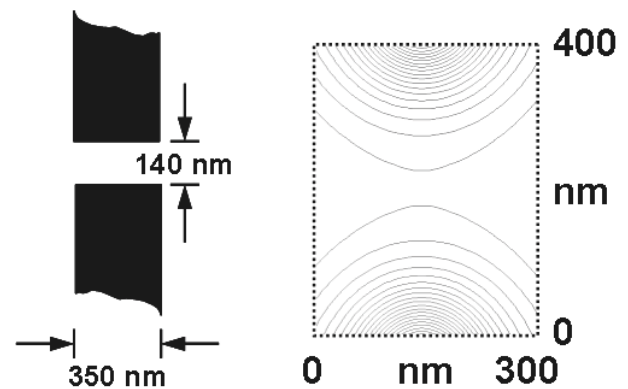


Figure 1: On the left, the split gates that form the model QPC. On the right, the contours of the confining potential at the level of the 2DEG.

2. ACHIEVING SELF-CONSISTENCY IN A MODEL QPC

We model a QPC formed by split gates as shown in the right panel of Fig. 1. For the initial 2D confining potential generated by these gates, we have used the model potential

suggested by Timp [8] :

$$V_{conf}(x, y) = f\left(\frac{2x-l}{2z_0}, \frac{2y+w}{2z_0}\right) - f\left(\frac{2x+l}{2z_0}, \frac{2y+w}{2z_0}\right) + \quad (1)$$

$$f\left(\frac{2x-l}{2z_0}, \frac{-2y+w}{2z_0}\right) - f\left(\frac{2x+l}{2z_0}, \frac{-2y+w}{2z_0}\right)$$

where

$$f(u, v) = \frac{eV_g}{2\pi} \left[\frac{\pi}{2} - \tan^{-1}(u) - \tan^{-1}(v) + \tan^{-1}\left(\frac{uv}{\sqrt{1+u^2+v^2}}\right) \right]. \quad (2)$$

Here l and w are the lithographic width (350 nm) and gap (140 nm) between the electrodes, respectively, and V_g is the applied gate voltage. The vertical distance between the 2DEG and the gate, z , has been taken to be 70 nm. The left panel shows the contours of potential that arise for a $V_g = -0.55$ V in a domain at the very center of the QPC. It is over this domain, which is actually smaller than the assumed lithographic dimensions of the QPC, that the simulations are performed. We have found it is unnecessary to go further out from the center as the answers we obtain change very little after ~ 5 propagating modes are allowed at the outer boundaries of the simulation region.

Including self-consistent effects through the Kohn-Sham local spin-density functional method[9], the total potential for spin σ is given by:

$$V_{tot}^\sigma(x, y) = V_{conf} + V_H + V_{exch}^\sigma + V_{cor}^\sigma. \quad (3)$$

where V_H is the Hartree potential, V_{cor}^σ is the correlation potential for which we have used the expression derived by Tanatar and Ceperly[10] and V_{exch}^σ is the exchange potential as obtained by Stern[11]. Since there is only strong confinement in one direction, instead of a full two dimensional treatment of the problem, our approach was to break the QPC into a series of one dimensional slices perpendicular to the x axis, and solve for the self-consistent potentials of each slice *individually* using a method analogous to that originally developed for quantum wires. Following Berggren and Yakimenko[7], a weak Zeeman term ($g\mu_B B\sigma \sim 10^{-6}$ eV) is included in the first few iterations of each self-consistent loop to break the initial spin degeneracy.

3. CALCULATING THE CONDUCTANCE

In keeping with the results for the self-consistent potential, our conductance calculations are performed on a square finite-difference lattice with lattice constant, a . Position can thus be specified by integers: $x=ia$ and $y=ja$. The conductances for the two spin orientations are computed separately. Keeping only the lowest order terms in the approximations of the derivatives, the 2D Schrödinger equation for electrons of spin σ becomes :

$$\begin{aligned} & -t(\psi_{i+1,j}^\sigma + \psi_{i-1,j}^\sigma + \psi_{i,j+1}^\sigma + \psi_{i,j-1}^\sigma) + (V_{i,j}^\sigma + 4t)\psi_{i,j}^\sigma \\ & = E^\sigma \psi_{i+1,j}^\sigma, \text{ where } t = \frac{\hbar^2}{2m^* a^2}, \end{aligned} \quad (4)$$

where $V_{i,j}^\sigma$ represents the discretized of the full potential at site i,j and E^σ is the energy. Since we are interested in current flow through the QPC, the situation which we consider is one in which the device is enclosed inside an ideal quantum wire, which extends outward to $\pm\infty$ along the x -axis. To calculate the transmission through a device, the modes are injected from the left side only with unit amplitude. Using (4), one can derive a transfer-matrices equation that relates adjacent slices to achieve this purpose. For a structure N slices long, one must thus solve the transfer matrix problem:

$$\begin{bmatrix} \mathbf{t}^\sigma \\ \mathbf{0} \end{bmatrix} = \mathbf{T}_0^{-1} \mathbf{T}_N \mathbf{T}_{N-1} \cdots \mathbf{T}_1 \mathbf{T}_0 \begin{bmatrix} \mathbf{I} \\ \mathbf{r}^\sigma \end{bmatrix}, \quad (5)$$

where \mathbf{t}^σ is a matrix of transmission amplitudes of waves exiting from the right part of the structure, and \mathbf{r}^σ is the matrix of amplitudes of waves reflected back towards the left. Given \mathbf{t}^σ , one calculate the conductance, G^σ , using the Landauer-Buttiker formula:

$$G^\sigma = \frac{2e^2}{h} \sum_{m,n} \frac{v_n^\sigma}{v_m^\sigma} |t_{m,n}^\sigma|^2 \quad (6)$$

where $t_{n,m}$ represents the transmission amplitude of mode n to mode m and the summation is only over propagating modes. The v 's are the mode velocities, which can be obtained by taking the expectation value of the current operator. Unfortunately, equation (5) in its current form is made numerically unstable by the exponentially growing and decaying contributions of the evanescent modes that accumulate when the product of transfer matrices is taken. Usuki *et al.*[12] overcame this difficulty by rewriting the transfer matrix problem in terms of an iterative scheme. The numerical stability of the Usuki *et al.* method in large part stemmed from the fact that the scheme involved products of some of the original matrices with matrices that were *inverted*, which tends to cancel out most of the troublesome exponential factors.

4. RESULTS

In Fig. 2, we plot the *total* conductance (the sum over the two spin channels) vs. V_g for a series of 1D electron densities, n_{1D} . These densities, set at left boundary of the simulation domain, are related to the Fermi energy, E_F , through

$$n_{1D} = \sum_{\sigma,m} (2m^* (E_F - E_m^\sigma) / \hbar)^{1/2} / \pi, \quad (6)$$

where E_m^σ are the energies of the modes and the sum is

restricted over those that propagate. Given n_{1D} , one can determine E_F which in turn can be converted to a 2D density. Thus, one can choose n_{1D} to yield reasonable with typical experimental measured values of the latter quantity. Here, the different curves correspond to different one-dimensional electron densities: $1.68 - 2.38 \times 10^6 \text{ cm}^{-1}$ ($E_F = 12.9 - 14.0 \text{ meV}$), from right to left respectively. For the confining potential considered, there are no actual conductance plateaus at $2 G_0$, only points of inflection in the conductance traces in that region, which shift according to the density. At $\sim G_0$, some traces show an actual plateau, while others develop a hump that falls somewhat short of this value, which can even drop below $\sim 0.5 G_0$ as the density is varied. Many individual traces have pairs of features below $\sim G_0$ and $\sim 0.5 G_0$, respectively.

In Fig.3, the conductance is plotted for a single density, $n_{1D} = 1.96 \times 10^6 \text{ cm}^{-1}$. This trace has a hump-like plateau at $\sim 0.8 G_0$ and a point of inflection at $\sim 0.3 G_0$. The contributions from spin-up and spin-down channels to the total conductance are also plotted. As is evident, the spin-down contribution initially dominates the conductance (dotted line), even up to almost G_0 . The implication is that *two* spin-down modes can be almost fully transmitted through the QPC in this case before the first spin-up mode makes it through. Insight into the different transmission characteristics can be obtained by looking at the self-consistent QPC potentials seen by the two spins. In the panels below, three pairs of potentials corresponding to gate voltages -0.50 V (i), -0.49 V (ii) and -0.47 V (iii) are shown.

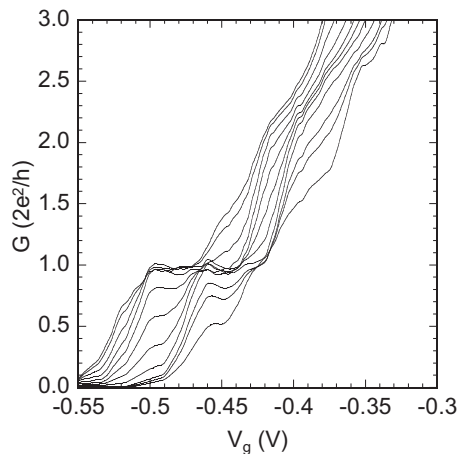


Figure 2: Total conductance vs. V_g for a series of electron densities.

Looking the insets, we see that compared with Fig. 1, an additional potential barrier structure becomes superimposed on top of the QPC when self-consistency is introduced, a structure that depends on whether the spin is up or down. This structure tends to weaken as more modes are allowed to pass through the QPC (note that the additional barriers are barely visible in panel (iii), which corre-

sponds to $2 G_0$). Since the spin dependent barriers shown in the insets of the lower three panels of Fig. 3 show relatively little variation along the y -direction, one can think of them as essentially quasi-one-dimensional. In the main parts of the lower three panels we adopt this point of view and plot the spin dependent potential averaged in the y -direction, $\langle V(x, y=y_0) \rangle$ vs. x for the three cases. Here, y_0 is the center of the QPC.

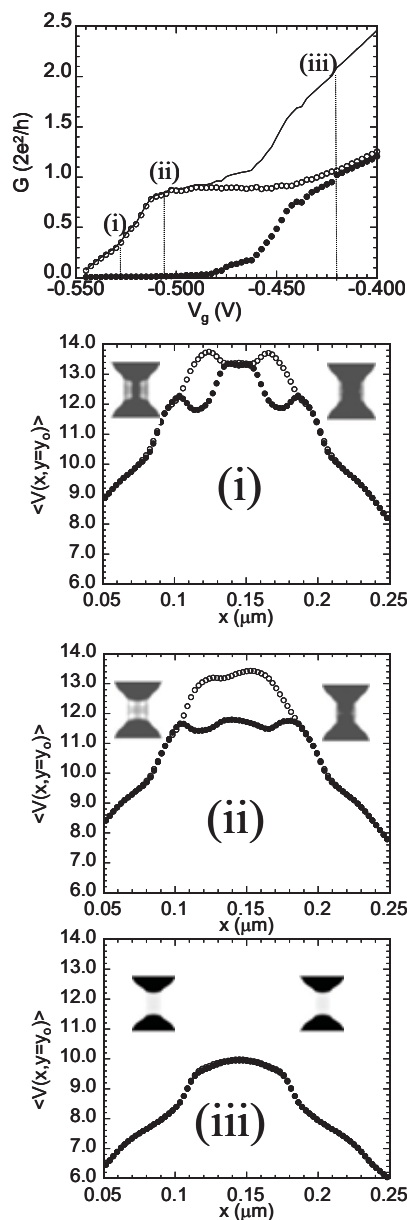


Figure 3: QPC conductance for a one-dimensional density, $n_{1D} = 1.96 \times 10^6 \text{ cm}^{-1}$ ($E_F = 13.4 \text{ meV}$). The solid line is the total conductance variation, while the black and open circles show the spin-up and spin-down contributions to the conductance. The self-consistent potentials for spin-down (left insets) and spin-up (right insets) at the indicated points are plotted below, along with the averaged potentials.

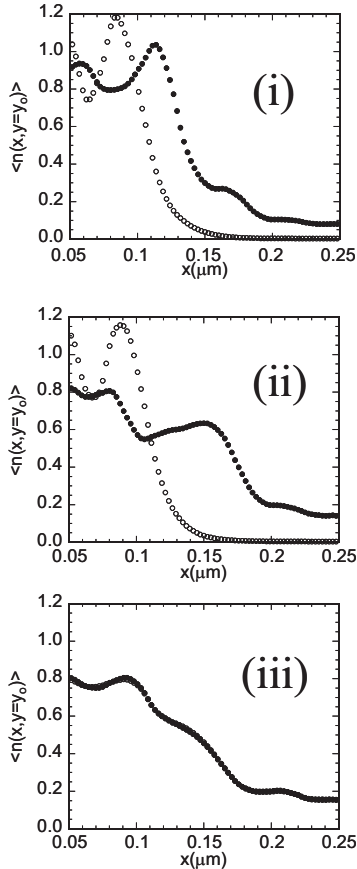


Figure 4: The average density along the x -direction is plotted for spin-up (open circles) and spin-down (black circles) for the three cases discussed above.

For case (i), the spin-down and spin-up potentials line up at the center of the QPC. However, away from the center, they deviate, with spin-down dropping significantly below spin-up, splitting with the latter and developing “shoulders”. Previously noted in the context of quantum wires[13], this potential splitting, *which can be larger than the level spacing of the modes*, is largely the result of the exchange potential and will oscillate as a function of the local density. The result of is that spin-down sees a tunneling barrier that is essentially the same height, but is much narrower. These barriers allow for the partial transmission of a single spin-down mode, but completely blocks spin-up modes from getting through. This effect can be seen in the top panel of Fig. 4, in which the average density along the QPC is plotted. For (ii), the spin-up barrier remains comparatively high, but the central portion of the spin-down barrier has now collapsed to the level of the “shoulders”. With this collapse, the first spin-down mode is allowed to be fully transmitted and large portions of a second mode now also make through the barrier, yielding the $\sim 0.8G_0$ conductance in this case (note the higher spin-

down density of the right in panel (ii) of Fig. 4). Meanwhile, the spin-up modes are still blocked. As V_g is reduced and the QPC is allowed to become more open, the spin-down and spin-up barriers gradually start moving back together again, with the spin-up modes gradually being transmitted through the QPC. By (iii), they have fully converged. Since the potential splitting effect noted earlier is known to eventually vanish at large densities, this convergence is not unexpected. Despite this, it is evident that the self-consistent potential is still has the form of an *extra* barrier superimposed over the initial QPC confining potential. *Its presence prevents modes from being cleanly transmitted through the QPC.* This is why the conductance only shows an inflection point at $2G_0$ rather than a fully formed plateau.

In conclusion, as in recent experiments, our SDFT calculations yield additional structure besides the standard conductance plateaus at integer values of G_0 . These can be accounted for by the formation of density and spin dependent barriers in the QPC region which can act as spin filters. The barriers themselves are rather generic features, however, a major effect of changing n_{1D} is to change their relative transparency. This is why Fig. 1 shows plateaus shifting and evolving for different values of n_{1D} .

REFERENCES

- [1] B. J. van Wees, H. van Houten, C. W. J. Beenakker, J. G. Williamson, L. P. Kouwenhoven, D. van der Marel, and C. T. Foxon, Phys. Rev. Lett. 60, 848 (1988).
- [2] M. Büttiker, Phys. Rev. B 41, 7906 (1990).
- [3] K. J. Thomas, J. T. Nicholls, M. Y. Simmons, M. Pepper, D. R. Mace, and D. A. Ritchie, Phys. Rev. Lett. 77, 135 (1996).
- [4] P. Ramvall, N. Carlsson, I. Maximov, P. Omling, L. Samuelson, W. Seifert, and Q. Wang, Appl. Phys. Lett. 71, 918-920 (1997).
- [5] K. Hirose, Y. Meir, and N. S. Wingreen, Phys. Rev. Lett. 90, 026804 (2003).
- [6] K.-F. Berggren and I. I. Yakimenko, Phys.Rev. B 66, 085323 (2002)
- [7] A. Shailos, R. Akis, J. P. Bird, S. M. Goodnick, D. K. Ferry, M. P. Lilly, J. L. Reno, and J. A. Simmons, unpublished.
- [8] G. Timp, Semiconductors and Semimetals, 35, 113 (1992).
- [9] W. Kohn and L.J. Sham, Phys. Rev. 140, A1133 (1965).
- [10] B. Tanatar, D.M. Ceperly, Phys. Rev. B 39, 505 (1989).
- [11] F. Stern, Phys. Rev. Lett., 30, 278 (1973).
- [12] T. Usuki, M. Saito, M. Takatsu, R.A. Kiehl, and N. Yokoyama, Phys. Rev. B, 52, 8244 (1995).
- [13] C.-K. Wang, and K.-F. Berggren, Phys. Rev. B 54, 4413 (1996).